CIVIL AND ENVIRONMENTAL ENGINEERING REPORTS

No. 1 2005

ELASTIC ANALYSIS OF THIN FIBER-REINFORCED PLATES

Mieczysław KUCZMA, Krzysztof KULA
University of Zielona Góra, prof. Z. Szafrana St. 2,
65-516 Zielona Góra, Poland

This paper is concerned with the bending problem of a fibre-composite plate in the elastic range. Within the classical Kirchhoff plate theory, two approaches are utilized. In the model due to Świtka, the fibre-composite plate is treated as a homogeneous medium with a number of embedded families of fibres, while in the second model the plate is considered as a system of orthotropic layers. The bending problem is formulated in classical and variational forms and solved by finite element method. We have developed our own computer code and numerically compared predictions of the two models and other models available in the program ABAQUS on test examples. Numerical results illustrating influence of the placement of fibres on the quantities of interest are also included.

Key words: fibre-composite layered plate, bending of anisotropic plate, finite element method, elastic solution

1. INTRODUCTION

A composite material is formed when two or more materials are combined. The properties of the composite are different, usually better then its individual components. This paper deals with the problem of bending of laminated composite plates, including fibre-composite plates. The analysed composite plate consists of the matrix, which is made of a modern plastic material, and a set of regularly disposed fibres made of glass or titan, for example. The bending problem of composite plates has been studied in many works, see e.g. [2, 3, 4, 6]. A finite element method formulation of the model suggested in [4] is given in [5].

The properties of a composite dependent on the properties of the constituent materials, and their distribution and interaction. In this paper we have

ISBN 83-89712-71-7

treated the composite plate as a fibre-composite plate (model of Świtka) and as a system of layers (a layerwise model). We have based our analysis on the basic assumptions of classical Kirchhoff plate theory.

Our aim in this is twofold; firstly, to develop our own computer program for anisotropic plates and to test it on typical examples, secondly we want to analyse the influence of the fibre orientation on the plate deflection and the plate bending and twisting moments. In the sequel, we shall briefly present two models for an anisotropic plate, constitutive relations for an orthotropic layer and next formulate the bending problem in classical and variational forms and its FEM approximation. We have developed our own computer code and numerically compared predictions of the model by Świtka and the layerwise model and other models available in the program ABAQUS on test examples. Numerical results illustrating influence of the placement of fibres on the quantities of interest are also included. The obtained results

2. THIN ANISOTROPIC PLATE

The differential equation for a thin anisotropic plate in bending takes the form

$$D_{11}\frac{\partial^4 w}{\partial x^4}+\left(2D_{12}+4D_{66}\right)\frac{\partial^4 w}{\partial x^2\partial y^2}+D_{22}\frac{\partial^4 w}{\partial y^4}+ 4D_{16}\frac{\partial^4 w}{\partial x^3\partial y}+4D_{26}\frac{\partial^4 w}{\partial x\partial y^3}=p \tag{1}$$

wherein $w=w(x,y)$ is the displacement of the middle plane of the plate $\Omega\subset R^2$, $p=p(x,y)$ is the load on the plate, and coefficients D_{ij} represent the plate bending and twisting stiffness,

$$\mathbf{D}=\begin{bmatrix} D_{11} & D_{12} & D_{16} \\ D_{12} & D_{22} & D_{26} \\ D_{16} & D_{26} & D_{66} \end{bmatrix} \tag{2}$$

2.1. The model of Świtka

The cross-section of the analysed fibre-composite plate is shown in fig.1 in which, for clarity, only one *r*th family of fibres is shown.

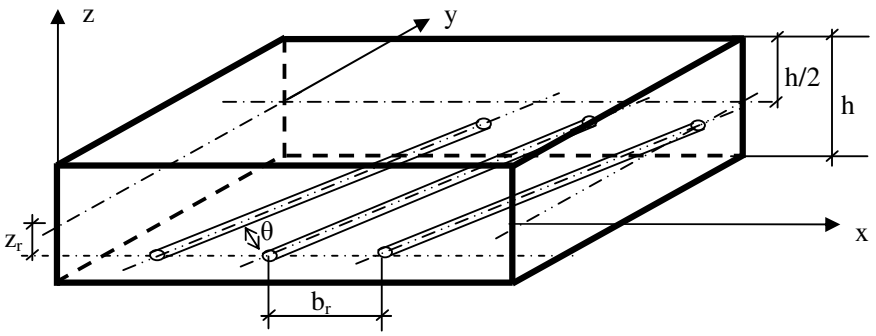

Fig.1. Fibre composite plate with one family of fibres

The differential equation for a fibre-composite plate in bending takes the form

$$D\nabla^4 w + \left[\sum_r \frac{E_r A_r}{b_r} z_r^2 s_i^r s_j^r s_k^r s_l^r - \sum_r \frac{E_r A_r}{b_r} z_r s_i^r s_j^r s_p^r s_q^r \sum_s c_{pq}^s z_s s_k^s s_l^s \right] w_{,ijkl} = p \tag{3}$$

Having compared coefficients of eqns. (1) and (3) we arrive at the following relationships (4):

$$D_{11} = D + \sum_r \frac{E_r A_r}{b_r} z_r^2 \left(s_1^r\right)^4 - \sum_r \frac{E_r A_r}{b_r} z_r \left(s_1^r\right)^2 s_p^r s_q^r \sum_s c_{pq}^s z_s \left(s_1^s\right)^2$$

$$D_{22} = D + \sum_r \frac{E_r A_r}{b_r} z_r^2 \left(s_2^r\right)^4 - \sum_r \frac{E_r A_r}{b_r} z_r \left(s_2^r\right)^2 s_p^r s_q^r \sum_s c_{pq}^s z_s \left(s_2^s\right)^2 \tag{4}$$

$$D_{12} = \nu_m D + \sum_r \frac{E_r A_r}{b_r} z_r^2 \left(s_1^r\right)^2 \left(s_2^r\right)^2 - \frac{1}{4} \sum_r \frac{E_r A_r}{b_r} z_r \left(s_1^r\right)^2 s_p^r s_q^r \sum_s c_{pq}^s z_s \left(s_2^s\right)^2 -$$
$$- \frac{1}{4} \sum_r \frac{E_r A_r}{b_r} z_r \left(s_2^r\right)^2 s_p^r s_q^r \sum_s c_{pq}^s z_s \left(s_1^s\right)^2$$

$$D_{66} = \frac{(1-\nu_m)D}{2} + \sum_r \frac{E_r A_r}{b_r} z_r^2 \left(s_1^r\right)^2 \left(s_2^r\right)^2 - \frac{1}{4} \sum_r \frac{E_r A_r}{b_r} z_r s_1^r s_2^r s_p^r s_q^r \sum_s c_{pq}^s z_s s_1^s s_2^s$$

$$D_{26} = \sum_r \frac{E_r A_r}{b_r} z_r^2 s_1^r \left(s_2^r\right)^3 - \frac{1}{4}\sum_r \frac{E_r A_r}{b_r} z_r s_2^r s_2^r s_p^r s_q^r \sum_s c_{pq}^s z_s s_1^s s_2^s - \\ - \frac{1}{4}\sum_r \frac{E_r A_r}{b_r} z_r s_2^r s_1^r s_p^r s_q^r \sum_s c_{pq}^s z_s s_2^s s_2^s \tag{4}$$

$$D_{16} = \sum_r \frac{E_r A_r}{b_r} z_r^2 \left(s_1^r\right)^3 s_2^r - \frac{1}{4}\sum_r \frac{E_r A_r}{b_r} z_r s_1^r s_1^r s_p^r s_q^r \sum_s c_{pq}^s z_s s_1^s s_2^s - \\ - \frac{1}{4}\sum_r \frac{E_r A_r}{b_r} z_r s_1^r s_2^r s_p^r s_q^r \sum_s c_{pq}^s z_s s_1^s s_1^s$$

in which

$$D = \frac{E_m h^3}{12\left(1-\nu_m{}^2\right)}, \qquad \mathbf{c}^r = col\left(c_{11}^r, c_{12}^r, c_{22}^r\right) = \frac{E_r A_r}{b_r}\mathbf{K}^{-1}\mathbf{s}^r, \qquad \mathbf{K} = \left\lfloor k_{ij} \right\rfloor_{3x3}$$

$$k_{11} = \frac{E_m h}{1-\nu_m{}^2} + \sum_r \frac{E_r A_r}{b_r}\left(s_1^r\right)^4, \qquad k_{12} = 2\sum_r \frac{E_r A_r}{b_r}\left(s_1^r\right)^3 s_2^r$$

$$k_{13} = \frac{E_m h \nu_m}{1-\nu_m{}^2} + \sum_r \frac{E_r A_r}{b_r}\left(s_1^r\right)^2\left(s_2^r\right)^2, \qquad k_{22} = 2\left[\frac{E_m h}{1+\nu_m} + 2\sum_r \frac{E_r A_r}{b_r}\left(s_1^r\right)^2\left(s_2^r\right)^2\right]$$

$$k_{23} = 2\sum_r \frac{E_r A_r}{b_r}\left(s_2^r\right)^3 s_1^r, \qquad k_{33} = \frac{E_m h}{1-\nu_m{}^2} + \sum_r \frac{E_r A_r}{b_r}\left(s_2^r\right)^4$$

with notations: E_m is the modulus of elasticity of the matrix, ν_m - Poisson's ratio of the matrix, h - thickness of the plate, E_r - the modulus of elasticity of the rth family of fibres, A_r - cross-sectional area of an individual fibre, z_r - the distance of the fibres of the rth family from the middle plane of the plate, b_r - spacing of the rth family of the fibres, s_1^r - cosine of angle between x-axis and axis of rth family of fibres, s_2^r - cosine of angle between y-axis and axis of rth family of fibres.

2.2. The layerwise model

The stiffness coefficients D_{ij} for the layerwise model are defined by

$$D_{ij} = \frac{1}{3}\sum_{k=1}^{N} \tilde{C}_{ij}^{(k)}\left(z_{k+1}^3 - z_k^3\right) \tag{5}$$

The cross-section of the analysed layered plate is shown in fig.2, where only two layers are marked for clarity. Location of the typical *k*th layer and its thickness h_k are defined by the coordinates z_k and z_{k+1}. A typical fibre layer is shown in fig. 3. All such layers are assumed to be orthotropic in their material coordinate systems $x_1\ x_2\ x_3$. The global coordinate system, in which the corresponding boundary problem is solved, is denoted by $x\ y\ z$.

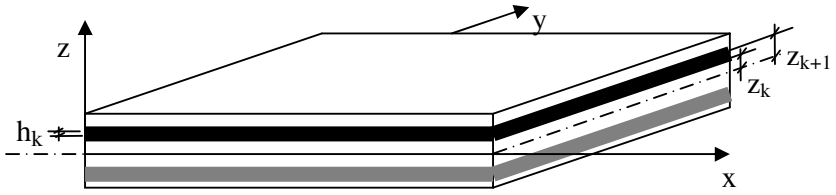

Fig. 2. Layered plate

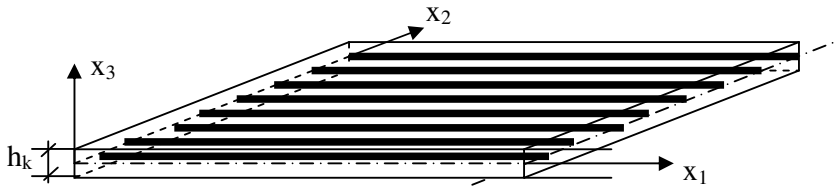

Fig. 3. Typical *k*th layer of fibre-composite plate, *k=1,2...N*

The constitutive equations between stress $\boldsymbol{\sigma}^{(k)}$ and strain $\boldsymbol{\varepsilon}^{(k)}$ tensors for the *k*th orthotropic layer in the material coordinate system $x_1\ x_2\ x_3$ may be written as

$$\boldsymbol{\sigma}^{(k)} = \mathbf{C}^{(k)}\boldsymbol{\varepsilon}^{(k)}$$

$$\begin{bmatrix}\sigma_{11}\\ \sigma_{22}\\ \sigma_{12}\end{bmatrix}^{(k)} = \begin{bmatrix}C_{11} & C_{12} & 0\\ C_{12} & C_{22} & 0\\ 0 & 0 & C_{66}\end{bmatrix}^{(k)} \begin{bmatrix}\varepsilon_{11}\\ \varepsilon_{22}\\ 2\varepsilon_{12}\end{bmatrix}^{(k)}$$

where

$$C_{11} = \frac{E_1}{1-\nu_{12}\nu_{21}} \qquad C_{22} = \frac{E_2}{1-\nu_{12}\nu_{21}}$$

$$C_{12} = C_{21} = \frac{\nu_{12}E_2}{1-\nu_{12}\nu_{21}} = \frac{\nu_{21}E_1}{1-\nu_{12}\nu_{21}} \qquad C_{66} = G_{12}$$

$$G_r = \frac{E_r}{2(1+\nu_r)} \qquad G_m = \frac{E_m}{2(1+\nu_m)}$$

$$E_1 = c_r E_r + c_m E_m \qquad E_2 = \frac{E_r E_m}{c_r E_r + c_m E_m}$$

$$\nu_{12} = c_r \nu_r + c_m \nu_m \qquad G_{12} = \frac{G_r G_m}{c_r G_r + c_m G_m}$$

Here: E_r - the modulus of elasticity of rth family of fibres (placed in kth layer), ν_r - Poisson's ratio of rth family of fibres, c_r - volume fraction of rth family of fibres, E_m - the modulus of elasticity of matrix, ν_m - Poisson's ratio of matrix, c_m - volume fraction of matrix.

The orthotropic constitutive equations become anisotropic in the global coordinate system. The anisotropy is characterised by matrix $\tilde{\mathbf{C}}^{(k)}$ and we have

$$\tilde{\boldsymbol{\sigma}}^{(k)} = \tilde{\mathbf{C}}^{(k)} \tilde{\boldsymbol{\varepsilon}}^{(k)}$$

$$\begin{bmatrix} \boldsymbol{\sigma}_{xx} \\ \boldsymbol{\sigma}_{yy} \\ \boldsymbol{\sigma}_{xy} \end{bmatrix}^{(k)} = \begin{bmatrix} \tilde{C}_{11} & \tilde{C}_{12} & \tilde{C}_{16} \\ \tilde{C}_{12} & \tilde{C}_{22} & \tilde{C}_{26} \\ \tilde{C}_{16} & \tilde{C}_{26} & \tilde{C}_{66} \end{bmatrix}^{(k)} \begin{bmatrix} \boldsymbol{\varepsilon}_{xx} \\ \boldsymbol{\varepsilon}_{yy} \\ 2\boldsymbol{\varepsilon}_{xy} \end{bmatrix}^{(k)}$$

$$\tilde{\mathbf{C}}^{(k)} = \mathbf{T}^{(k)} \mathbf{C}^{(k)} \left(\mathbf{T}^{(k)}\right)^T$$

where $\mathbf{T}^{(k)}$ is the transformation matrix from the material coordinate system to the global coordinate system

$$\mathbf{T}^{(k)} = \begin{bmatrix} \cos^2\theta & \sin^2\theta & -2\sin\theta\cos\theta \\ \sin^2\theta & \cos^2\theta & 2\sin\theta\cos\theta \\ \sin\theta\cos\theta & -\sin\theta\cos\theta & \cos^2\theta - \sin^2\theta \end{bmatrix}$$

with $\theta = \theta_k$ being the angle between x and x_1 for the kth layer.

3. VARIATION FORMULATION

Equation (1) should be supplemented with appropriate boundary conditions. For the solution of (1) in practical problems one has to resort to approximate, numerical methods. We have used the finite element method which allows one to effectively solve complex boundary value problems (BVPs) of mechanics. To this aim we first formulate the BVP for (1) in a variational form. Let $U \subset H^2(\Omega)$ be a set of kinematically admissible displacements of the plate, $V \subset H^2(\Omega)$ a set of testing functions (virtual displacements). By $H^2(\Omega)$ we designate the Hilbert space of functions that are square integrable with up to their second derivative on Ω. Further, let Γ denote the boundary of Ω and $\Gamma = \Gamma_D \cup \Gamma_N \quad \Gamma_D \cap \Gamma_N = 0$, Γ_D being the part of the boundary where constraints on displacements are imposed and on Γ_N - stress boundary conditions. The weak (variational) formulation of the BVP for (1) may be obtained from the principle of virtual work and stated as follows.

Find $w \in U$ such that

$$a(w,v) = f(v) \qquad \text{for all} \quad v \in V \tag{6}$$

The bilinear form $a(\bullet,\bullet)$ and the linear form $f(\bullet)$ are

$$a(w,v) = \int_{\Omega} \left(D_{11}\frac{\partial^2 w}{\partial x^2}\frac{\partial^2 v}{\partial x^2} + 2D_{12}\frac{\partial^2 w}{\partial x^2}\frac{\partial^2 v}{\partial y^2} + 4D_{16}\frac{\partial^2 w}{\partial x^2}\frac{\partial^2 v}{\partial x \partial y} + \right.$$
$$\left. + 4D_{26}\frac{\partial^2 w}{\partial x \partial y}\frac{\partial^2 v}{\partial y^2} + D_{22}\frac{\partial^2 w}{\partial y^2}\frac{\partial^2 v}{\partial y^2} + 4D_{66}\frac{\partial^2 w}{\partial x \partial y}\frac{\partial^2 v}{\partial x \partial y} \right) dxdy$$
$$f(v) = \int_{\Omega} pv dxdy + \int_{\Gamma_N} \left(M_{nn}\frac{\partial v}{\partial n} + M_{ns}\frac{\partial v}{\partial s} + Q_n v \right) ds$$

and correspond to the elastic strain energy and the virtual work of external loads, respectively.

4. FEM APPROXIMATION

In the finite element method the middsurface plane of the plate, Ω, is divided into a number of finite elements $\Omega^e \subset \Omega$, and within each element *e* the displacement field *w(x,y)* is approximated by $w^e(x,y)$. Then, the displacement *w* can be expressed as

$$w(x, y) \approx \sum_e w^e(x, y) = \sum_e \mathbf{N}^e(x, y)\, \mathbf{q}^e = \mathbf{N}\, \mathbf{q} \tag{7}$$

where $\mathbf{N}^e = \mathbf{N}^e(x, y)$ is the matrix of shape functions and $\mathbf{q}^e$ is the vector of the nodal parameters for element e, whereas $\mathbf{N}$ and $\mathbf{q}$ are their counterparts for the whole plate. Using (7) we can define stresses and strains in the plate as a function of $\mathbf{q}$:

– field of strains

$$\boldsymbol{\varepsilon} = \begin{bmatrix} \varepsilon_{xx} \\ \varepsilon_{yy} \\ \gamma_{xy} \end{bmatrix} = -z \begin{bmatrix} w_{,xx} \\ w_{,yy} \\ 2\, w_{,xy} \end{bmatrix} = -z\, \boldsymbol{\kappa} = -z\, \mathbf{B}\, \mathbf{q} \tag{8}$$

where $\boldsymbol{\kappa}$ stand for the matrix of curvatures

$$\boldsymbol{\kappa} = \begin{bmatrix} \kappa_{xx} \\ \kappa_{yy} \\ 2\kappa_{xy} \end{bmatrix} = \mathbf{B}\, \mathbf{q}, \qquad \mathbf{B} = \boldsymbol{\partial}\mathbf{N}, \quad \partial = \begin{bmatrix} \partial^2/\partial x^2 \\ \partial^2/\partial y^2 \\ 2\partial^2/\partial x \partial y \end{bmatrix} \tag{9}$$

– field of stresses in kth layer

$$\boldsymbol{\sigma}^{(k)} = \begin{bmatrix} \sigma_{xx} \\ \sigma_{yy} \\ \sigma_{xy} \end{bmatrix}^{(k)} = \tilde{\mathbf{C}}^{(k)}\, \boldsymbol{\varepsilon}^{(k)} = -z\, \tilde{\mathbf{C}}^{(k)}\, \mathbf{B}\, \mathbf{q}, \quad z \in [z_k, z_{k+1}] \tag{10}$$

– field of moments

$$\mathbf{M} = \begin{bmatrix} M_{xx} \\ M_{yy} \\ M_{xy} \end{bmatrix} = -\mathbf{D}\, \mathbf{B}\, \mathbf{q} \tag{11}$$

The vector of nodal parameters $\mathbf{q}$ can be eventually determined from the system of the equilibrium equations

$$\mathbf{K}\, \mathbf{q} = \mathbf{f} \tag{12}$$

in which **K** is the global stiffness matrix and **f** is the global vector of nodal forces, both obtained by aggregation of all elemental contributions. In our own computer program we have used a 4-node quadrilateral finite element (PlQ4) with 12 degree of freedom (DOF). The explicit formulae for elements K_{ij} of the stiffness matrix for this quadrilateral finite element are listed in [1]. For the sake of comparison, we have calculated test examples both with our program and the ABAQUS software.

5. NUMERICAL EXAMPLES

In this section we have presented and compared some of the results of numerical tests we have obtained for fibre-reinforced plates when using different models and various types of finite elements. The influence of finite element meshes is also considered.

Exmaple 1.
At first we have analyzed a square simply supported orthotropic fibre-composite plate and compared the FEM results with the analytical Navier solution. The plate is reinforced by four families of fibres (see fig. 4). The thickness of the plate is 0.01 m and material coefficients are E_m=3,15 GPa, ν_m=0,38, E_r=85,5 GPa, ν_r=0,20.The plate is loaded by a uniformly distributed pressure q=1 kPa. We have solved the plate using the model of Świtka and the layerwise model, the corresponding stiffnesses D_{ij} are gathered in table 1. The used finite element was 20 x 20. The distribution of plate's deflection along half-span cross-section A-A for various cases is shown in fig.5. The solutions are similar with maximum differences of about 5%.

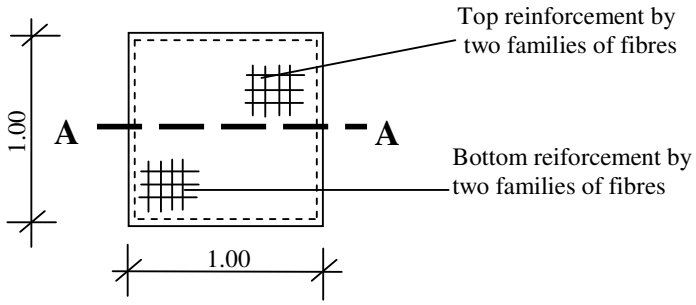

Fig. 4. Orthotropic fibre-composite plate

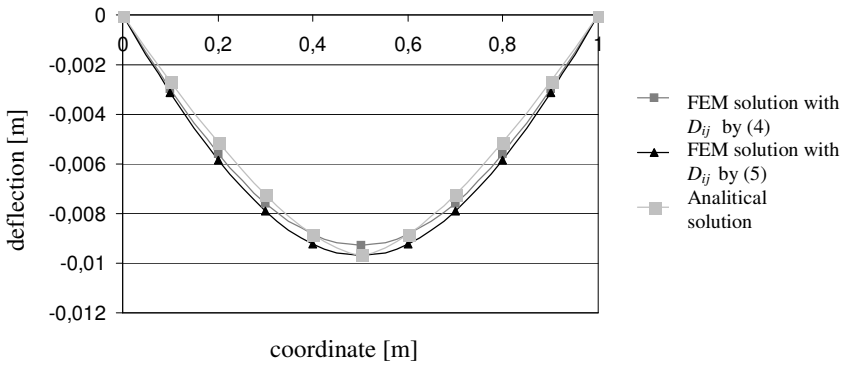

Fig. 5. Deflection along the cross-section A-A in an orthotropic plate (cf. fig.4)

	D_{11}	D_{12}	D_{22}	D_{66}
Model of Świtka	5.473E-4	1.166E-4	5.347E-4	9.511E-5
Layerwise model	5.541E-4	1.209E-4	5.426E-4	1.07E-4

Tab.1. Example 1: stiffness coefficients D_{ij} by two models, with $D_{16}=D_{26}=0$

Example 2.

Next, we have tested the fibre-composite plate that was composed of polyester matrix and eight families of glass S fibres. Figure 6 shows cross-section of this plate. In our tests some selected families of fibres are rotated from the global coordinate system by angle θ_i. The angle θ_i in the layerwise model is between global and material coordinate systems. Thickness of the plate is h=0.02 m and material coefficients are E_m=3,15 GPa, ν_m=0,38, E_r=85,5 GPa, ν_r=0,20. We solved two cases, C1 and C2, with different orientations of the fibre families (in all the cases the reinforcement is symmetric to the middsurface plane of the plate, M denotes a layer of matrix without fibres):

C1: [M/0/90/0+θ/90+θ/0/90/0+θ/90+θ/M]s,

C2: [M/0/90/22,5/112,5/45/135/67,5/157,5/M]s.

We have analyzed rectangular plate (1,00 m x 1,50 m) loaded by the uniformly distributed preassure (p=1 kPa) and concentrated force (P=1 kN) applied at the central point of the plate (point C). The plate is fixed on two edges and simply supported on one edge, see fig. 7. We have compared displacements in characteristic points B and C (fig.7) of the plate determined by own program and ABAQUS with different elements and meshes (figs. 8-11) using the layered model.

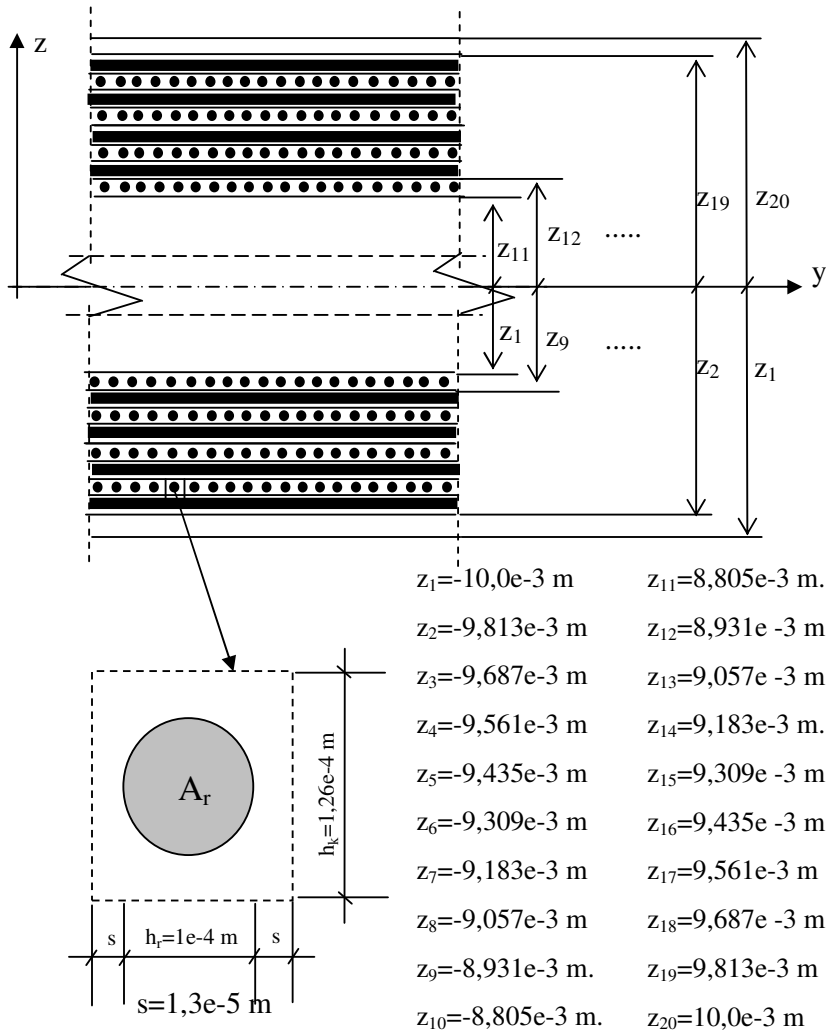

Fig. 6. Cross-section of the analysed plate and “cell” in layer with fibres

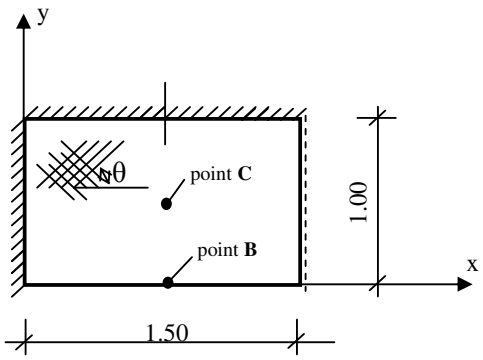

Fig.7. Examples 2 and 3: rectangular plate 1.00 x 1.50

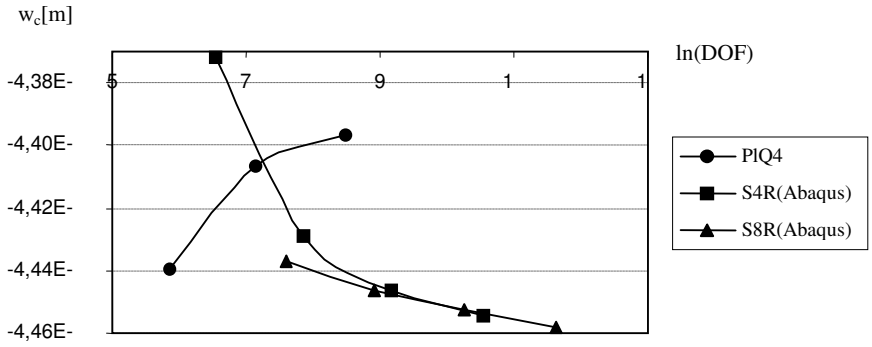

Fig.8. Case C1 ($\theta=0^{\circ}$): deflection at point C for different elements and meshes

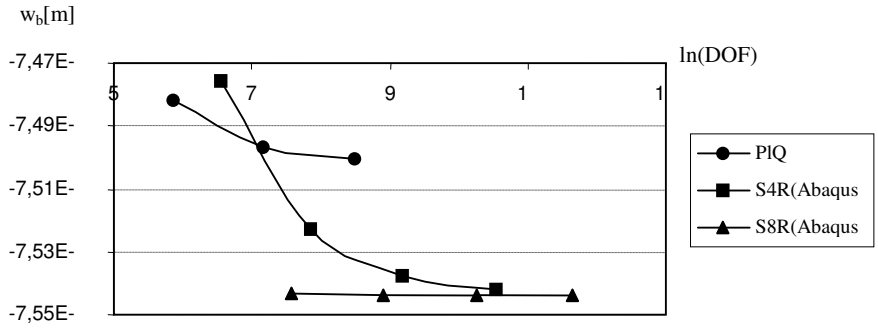

Fig.9. Case C1 ($\theta=0^{\circ}$): deflection at point B for different elements and meshes

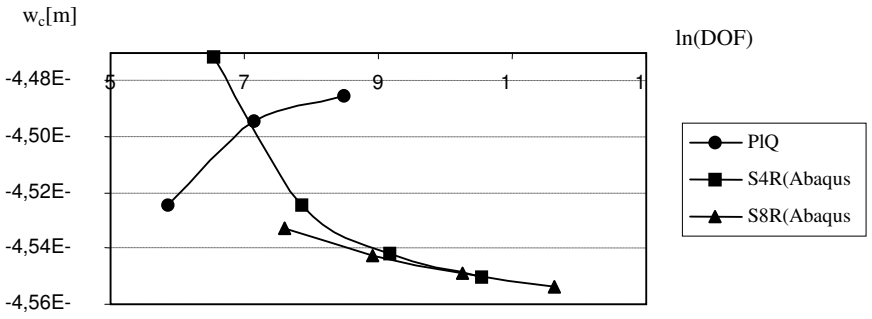

Fig.10. Case C2: deflection at point C for different elements and meshes

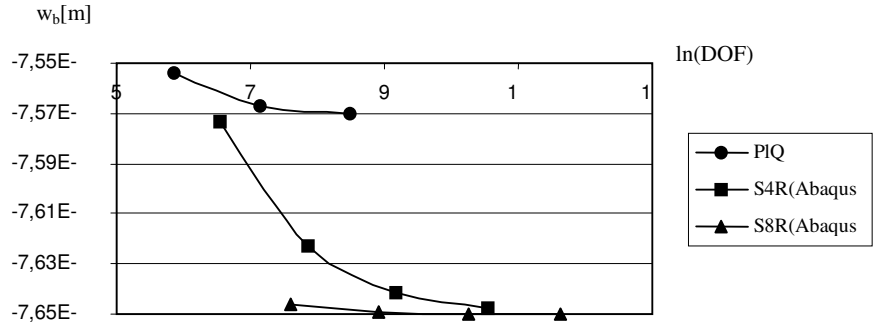

Fig.11. Case C2: deflection at point B for different elements and meshes

Example 3.

We have analyzed the same plate as in example 2, case 1: [M/0/90/0+θ/ 90+θ/ 0/90/0+θ/90+θ/M]s and solved it for various values of angle θ in the indicated layers. Figures 12 to 14 show the influence of θ on the coefficients of stiffness D_{ij} in both the models. Next, we analysed this influence on displacements (figs. 15-16) and stresses (figs. 17-20). It can be seen that although the differences in stiffnesses are about 13% in the case of D_{11} and about 40% in D_{12}, this is not to such extent reflected in displacements whose changes are less then 5%. Finally, figs. 17 and 18 illustrate distributions of shear stress σ_{xy} for two values of θ by means of level sets.

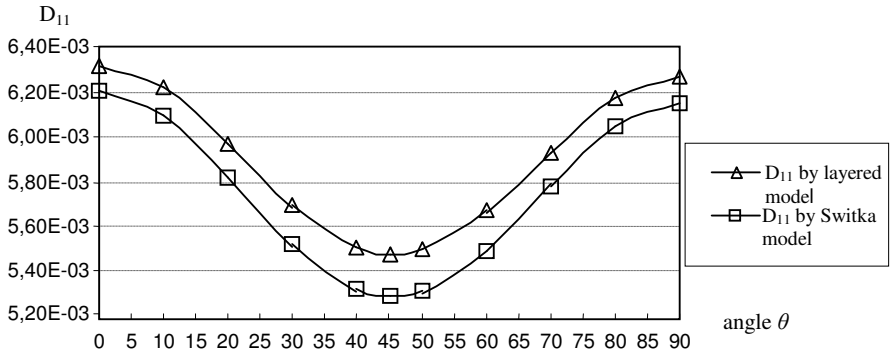

Fig.12. Influence of fibre orientation on D_{11} by different models

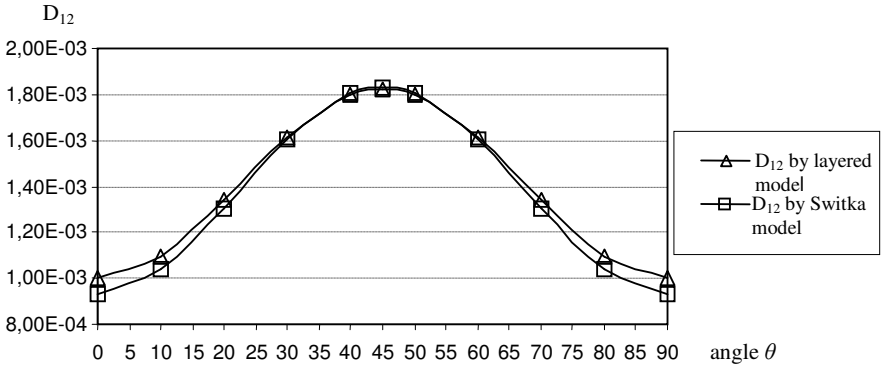

Fig.13. Influence of fibre orientation on D_{12} by different models

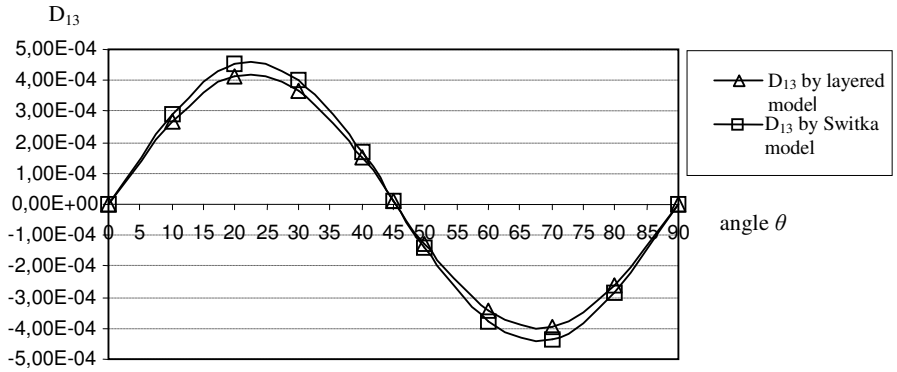

Fig.14. Influence of fibre orientation on D_{13} by different models

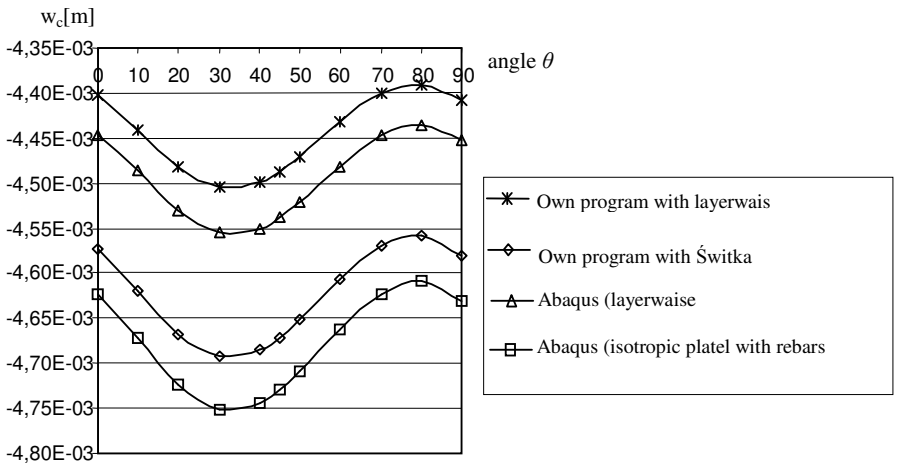

Fig.15. Case C1: influence of fibre orientation on deflection at point C by different models and programs

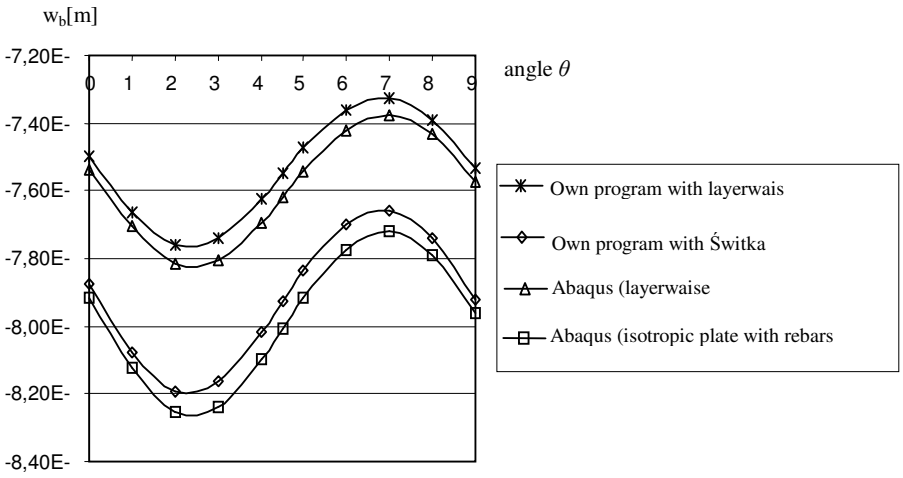

Fig.16. Case C1: influence of fibre orientation on deflection at point B by different models and programs

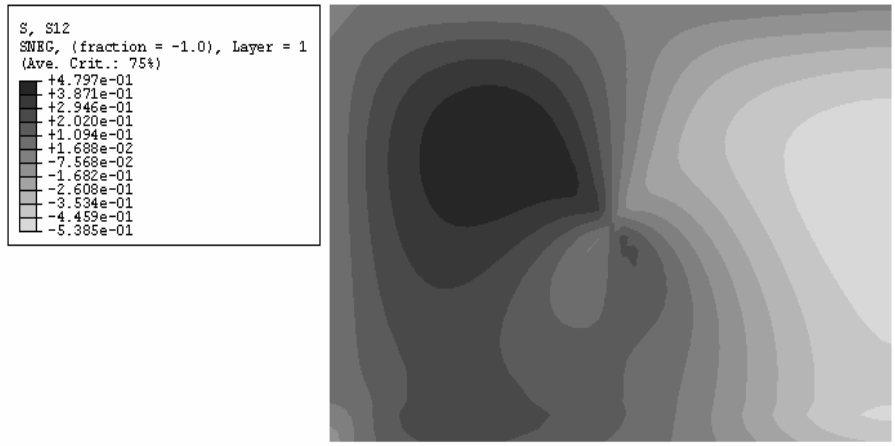

Fig.17. Case C1 (θ=0˚): Stress σ_{xy} on the bottom surface of plate

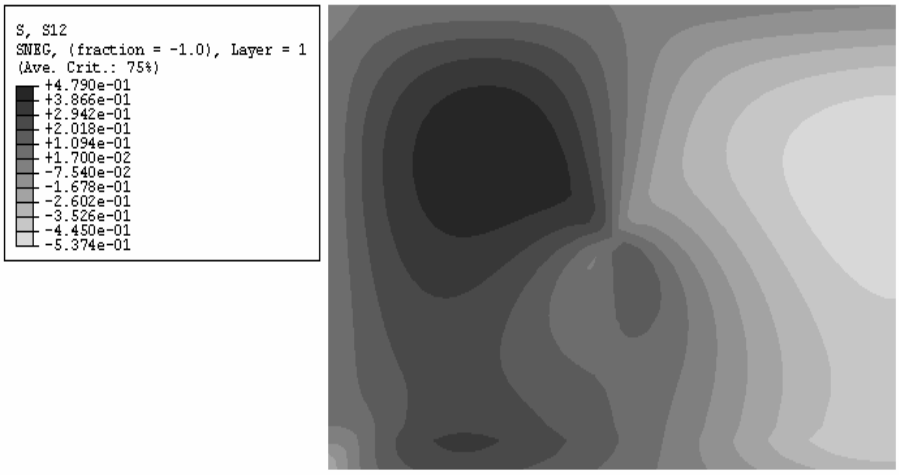

Fig.18. Case C1 (θ=45˚): stress σ_{xy} on the bottom surface of plate

6. CONCLUSION

In the paper we have presented the results of numerical simulation of the bending problem for a thin fibre-reinforced plate in the elastic range, making use of a number of models. The corresponding differential equation of the anisotropic plate is solved by the finite element method. In calculations we have used our own computer program and the program ABAQUS. The obtained results show some noticable differences in values of stiffness coefficients by the approach of Świtka and the layerwise approach, however, the resulting differences in displacements are of minor importance. If fact, the predictions of Świka's model are close to the results by ABAQUS with the rebar model. The applied 4-node quadrilateral plate element has proved to be quite effective, except for regions with point loads where the solution convergences in oppposite direction to that of ABAQUS. Finally, it may be concluded that the differences in the final quantities of interest due to the used different mathematical models of fiber-reinforcement are of minor importance from the enginnering point of view.

Acknowledgement
Work supported by the Committee for Scientific Research (KBN) under Grant No 5 T07A 042 24 in years 2003-2006. This support is gratefully acknowledged.

REFERENCES

1. Kuczma M.S., Kula K.*, Application of FEM in mechanics of fibre composite plates*. Problemy budownictwa. Zielona Góra 2003.
2. Lewiński T., Telega J.J., *Plates, Laminates and Shells*, World Scientific, Singapore 1999.
3. Reddy J.N., *Mechanics of laminated composite plates. Theory and analysis*, CRC Press 1997.
4. Świtka R., *Equations of the fibre composite plates*, Engng.Trans., 40, 2, 187-201, 1992.
5. Świtka R., Kuczma M.S., Kula K., *Analysis of elastic fibre-composite plates by FEM* (in Polish). Proc. VI-th Conference on Composite Structures, Zielona Góra 2002.
6. Woźniak Cz. (Ed.), *Mechanics of elastic plates and shells* (in Polish), PWN, Warszawa 2001.
7. ABAQUS 6.4, *Analisys User's Manual / CAE User's Manual,* USA 2003.

ANALIZA SPRĘŻYSTYCH PŁYT ZBROJONYCH WŁÓKNAMI

S t r e s z c z e n i e

W niniejszej pracy rozważa się zagadnienie zginania włóknokompozytowych płyt w zakresie sprężystym. Dla porównania, współczynniki sztywności płyty na zginanie i skręcanie wyznacza się według modelu Świtki i modelu warstwowego. Do wyznaczenia rozwiązania różniczkowego równania anizotropowej płyty zastosowano metodę elementtów skończonych. Rozwiązanie numeryczne wyznaczono za pomocą opracowanego własnego programu komputerowego i wykorzystując program ABAQUS celem dokonania porównania. Praca zawiera wyniki wielu analiz numerycznych, wskazujące na wpływ kierunku ułożenia włókien oraz zastosowanych elementów skończonych i gęstości siatki elementów na wielkości fizyczne.